Journal of CO2 Utilization 59 (2022) 101927

Contents lists available at ScienceDirect

Journal of CO2 Utilization

journal homepage: www.elsevier.com/locate/jcou

Exergoenvironmental analysis and thermoeconomic optimization of an industrial post-combustion CO_2 capture and utilization installation

Reza Shirmohammadi [a,*], Alireza Aslani [a], Roghayeh Ghasempour [a,*], Luis M. Romeo [b], Fontina Petrakopoulou [c]

[a] Department of Renewable Energies and Environment, Faculty of New Sciences & Technologies, University of Tehran, Tehran, Iran
[b] Escuela de Ingeniería y Arquitectura, Departamento de Ingeniería Mecánica, Universidad de Zaragoza, María de Luna 3, Zaragoza 50018 Spain
[c] Department of Thermal and Fluid Engineering, University Carlos III of Madrid, Madrid, Spain

ARTICLE INFO

Keywords:
CO_2 utilization
Optimization
Exergy
Exergoeconomic
Exergoenvironmental
CCU
LCA

ABSTRACT

CO_2 utilization is one of several tools available to us to mitigate climate change. This paper aims to study and optimize the urea production in the largest CO_2 utilization plant in Iran. The location, magnitude, and source of thermodynamic inefficiencies of the plant are evaluated using exergy, exergoeconomic and exergoenvironmental analyses. The optimization process uses as decision variables the temperature of the lean monoethanolamine solution and loading, along with the height of the absorber and the stripper of the plant. The decision variables and objective functions are trained with a hybrid combination of an artificial neural network with a genetic algorithm. The multi-objective genetic algorithm results in a pareto front of solutions. The exergy efficiency of the overall system is found to be 30.89% and 3.57, 2.86, 2.21% of the exergy of the fuel provided to the plant is destroyed in the soda ash wash direct contact, the stripper, and the absorber columns (424.07, 339.71 and 258.61 kW), respectively. The exergoeconomic analysis shows that the heat exchangers E-7 and E-8 result in relatively low exergoeconomic factor; therefore, an enhancement in the thermodynamic performance of the heat exchangers should be considered. The absorber column is found to have the largest environmental impact, equal to approximately 0.1205 mPt/s. The highest environmental impact of exergy destruction, equal to 33,256.3 mPts/hr is found in the stripper.

1. Introduction

Climate change is one of the most challenging environmental, social and economic threats of the last century [1]. Industries manily rely on fossil fuels for their operation, whereas renewables are capital-intensive, and their accessibility declines their competitiveness with fossil fuels [2]. Therefore, fossil fuels play a vital role in the future energy mix of the world specially in developing countries such as Iran. Iran is developing the greenhouse industry because of its high population growth, harsh and diverse climate, and the growing water crisis [3]. Carbon Capture, Utilization and Storage (CCUS) is an option to reduce greenhouse gas emissions. Even though the implication of such systems is recognized to battle climate change, its commercial large-scale application is yet to be realized, mainly due to its associated energy penalty [4,5]. There are three main categories of capture processes: post-combustion, pre-combustion and oxyfuel processes. Chemical absorption using amine solvents is the most advanced technology for post-combustion CO_2 capture [6]. The main method for CO_2 recovery is the absorption of the CO_2 in the flue gas of a power plant using an amine-based solvent; a process that is then followed by the desorption of the CO_2 and the regeneration of the solvent [7]. The most common amine that is often employed for CO_2 scrubbing processes, is Monoethanolamine (MEA). The main challenge in this kind of systems is to reduce the energy required for the regeneration of the solvent discussed in [8] and [9]. The thermal energy required to regenerate the solvent in post-combustion CCS is typically provided with low-pressure steam extracted from the plant which leads to some efficiency penalty [10]. The regeneration of the solvent and consequently the CO_2 recovery, is supported with heat transfer from low-pressure steam extracted from the power plant [11]. Table 1 shows important parameters of Post-combustion Carbon Capture (PCC) reported in similar systems in the literature.

More relevant studies on the evaluation of CO_2 capture systems include the application of exergy analysis [18]. Lara et al. [19] used the second law of thermodynamics to reduce the energy penalties of a CO_2 capture process. Atsonios et al. [20] applied exergy analysis to identify

* Corresponding authors.
E-mail addresses: r.shirmohammadi@ut.ac.ir, r.shirmohammadi1987@gmail.com (R. Shirmohammadi), ghasempour.r@ut.ac.ir (R. Ghasempour).

https://doi.org/10.1016/j.jcou.2022.101927
Received 16 December 2021; Received in revised form 24 January 2022; Accepted 3 February 2022
Available online 23 February 2022

Nomenclature

Abbreviations

ANN	Artificial Neural Network
CCU	Carbon Capture and Utilization
CCUS	Carbon Capture Utilization and Storage
EI	Environmental Impact
GA	Genetic Algorithm
LCA	Life Cycle Assessment
PFHE	Plate and Frame Heat Exchanger
TOPSIS	Technique for Order of Preference by Similarity to Ideal Solution

Symbols

b	specific environmental impact per exergy unit (mPts/kJ)
$\dot{B}_j$	environmental impact rate of material stream (mPts/s)
C	Cost (USD)
ex	Specific exergy (J/kg)
$\dot{E}_D$	Exergy destruction rate (kW)
$\dot{E}_f$	Fuel exergy rate (kW)
$\dot{E}_p$	Product exergy rate (kW)
h	Specific enthalpy (kJ/kg)
K	Component
$\dot{m}$	Mass flow rate (kg/s)
P	Pressure (kPa)
$\dot{Q}$	Rate heat transfer (kW)
R	Universal gas constant (kJ/kmol.K)
S	Specific entropy (kJ/kg.K)
T	Temperature (K)
V	Velocity (m/s)
$\dot{W}$	Work transfer rate (kW)
$\dot{Y}$	component related environmental impact rate (mPts/s)
$\dot{Z}$	Capital investment (USD)

Greek symbols

ε	Efficiency
φ	Maintenance factor
τ	Annual operating hours

Subscripts

0	Reference state condition (1 atm, 298 K)
1, 2, …, 116	Points in Fig. 1.
Ph	Physical exergy
Ch	Chemical exergy
D	Destruction
F	Fuel
P	Product
tot	Total

Superscripts

i	Number of components
n	Number of operation years

Table 1
Important parameters of PCC with MEA solvent.

Reference	Mol. fraction of CO_2 [%]	Mass fraction of Solvent [wt%]	Pressure of Stripper [bar]	Temperature of steam [°C]	Duty of reboiler [kJ/kgCO_2]	CO_2 final pressure [bar]	Efficiency of capture [%]
Shirmohammadi et al. [12]	11	30	3.3	150	3410	15	82
Ferrara et al. [13]	13	30	1.6	130	5112	152	90
Geuzebroek et al. [14]	3.5	30	N/A	140	4300	N/A	90
Amrollahi et al. [15]	3.8	30	1.86	145	N/A	110	90
Yu et al. [16]	12.6	30	N/A	296	N/A	130	90
Wang et al. [17]	14.4	30	2.1	296	4550	N/A	90

Table 2
Composition of the flue gas stream.

Substance	Mole fraction
N2	0.724
CO_2	0.0678
O2	0.0326
H2O	0.1756

the losses and evaluate the performance of diverse CO_2 capture technologies, i.e., amine scrubbing, calcium looping, and oxyfuel combustion for fossil fuel-fired power plants. Ferrara et al. [13] simulated chemical absorption using a MEA-based solvent with a capture rate of 90% in a coal-fired power plant. They analyzed the system using exergy and exergoeconomic analyses. They traced most irreversibilities in the components where the chemical capture of the CO_2 took place. An achieved improvement in the design of the plant reducing the unit cost of carbon capture from 35.0 to 31.8 US$/ton CO_2. Gatti et al. [21] applied thermodynamic analysis to study alternative structures of methanol absorption for acid gas removal to design a CO_2 capture unit. Valenti et al. [22] realized energy and exergy analyses of carbon capture using a chilled ammonia process. The chilled ammonia technology focus on reducing the energy use and solving corrosion and degradation issues.

Odejobi et al. [23] simulated a CCU plant for methanol production, and evaluated the system with an exergy analysis. They reported higher irreversibility in the CCU plant is occurred in the heat exchanger followed by the lean cooler and the stripper. Shirmohammadi et al. [12] realized a technoeconomic analysis of a natural gas-fired power generation system with CO_2 capture using MEA absorption. Most irreversibilities were found in the components where the chemical capture and release of the CO_2 were carried out, i.e., the CO_2 absorber and stripper. Yulia et al. [24] conducted a comprehensive study of coal-fired power generation system with CO_2 capture. They optimized the system to maximize the exergy efficiency and minimize the exergoenvironmental impact of the plant. They found relatively low exergy efficiencies for the heat exchangers, regenerators, and absorbers.

In this work, exergy, exergoeconomic, and exergoenvironmental analyses are used to identify the location, magnitude, and sources of thermodynamic inefficiencies and environmental impacts (EIs) in an integrated CO_2 capture and utilization unit. Finally, an artificial neural network (ANN) is used to train the data and a GA is used to optimize the process in terms of exergy efficiency and total cost of the system.

Table 3
Thermodynamic properties of the streams of the CCU plant.

Stream No.	Type of stream	Mass flow rate (Kg/s)	Temperature° C))	Pressure (bar)
1	Flue gas	17.58	178	**0.8776**
2	Flue gas	16.56	42	**0.8621**
3	Flue gas	16.56	47	**0.9007**
4	Vent	14.99	43	**0.8776**
7	H_2O-Na_2CO_3	26.82	42	**2.5**
8	Rich MEA	33.68	51.7	**1.4**
16	Rich MEA	33.68	57	**4.7**
17	Rich MEA	33.68	87	**4.4**
18	Semi-lean MEA	32.29	90	**3.8**
19	Semi-lean MEA	32.29	116	**3.6**
20	Lean MEA	32.13	126	**2.35**
21	Lean MEA	32.13	100	**2.15**
22	Lean MEA	32.13	70	**1.95**
23	Lean MEA	32.11	48	**1.75**
25	Captured CO_2	1.86	86	**2.2**
26	CO_2 (product)	1.57	43	**2**
27	Reflux (H_2O)	0.29	43	**2**
28	Drainage (H_2O)	28.40	65	**2.5**
29	Purge (H_2O)	17.58	43	**2**

2. Case study

Kermanshah Petrochemical Industries Co. (KPIC) manufactures and sells chemicals and agricultural fertilizers. The company produces urea fertilizers, liquid ammonia and nitrogen. In this petrochemical complex, a CCU was established to capture the carbon dioxide exhausted with the flue gas of the primary reformer of the ammonia plant. The composition of the flue gas is provided within Table 2. The captured CO_2 is then transferred to the compressor of the urea plant. This project was licensed, designed and realized by Shahrekord Carbon Dioxide Co. (SCD) to recuperate 132 Metric Tons Per Day (MTPD) of CO_2 from the flue gas. This technology has enabled KPIC to reduce its natural gas consumption by 21.1 Million of Normal Cubic Meters (M Nm^3) per year, and helps the company avoid over 40,000 tons of CO_2 emissions annually. Additionally, the production capacity has increased by 5%, without any additional investment [25].

3. Simulation framework and process description

The CCU plant is simulated via the chemical process simulator ASPEN Hysys® V. 10, using the Acid Gas Property Package models [26]. The CCU plant contains three columns, i.e., the soda ash wash-direct contact (SADCC), the absorption, and the stripper columns. The SADCC column contains of two packed sections with a height of 6 m and diameter of 3.8 m. The absorber contains 5 segments with a total height of 13 m. The cooling and washing sections are located at the top part and two intercoolers are placed in the middle section of the absorption column. The lean solvent is delivered to the third segment of the absorber, in which the absorption with the aqueous solution MEA takes place. Two intercoolers are located in the middle section of the absorption column to enhance the absorption rate. The rich solution is heated in the two-stage rich-lean heat exchangers. The rich solvent is then entered into the top segment of the stripper, in which the regeneration of solvent is being completed. The stream from the top of the stripper, containing high amount of CO_2, is delivered to the condenser in which the vaporized part is separated and quite pure CO_2 (with 95% molar concentration) is sent to the compressor of the urea plant [27,28]. Table 3 shows the thermodynamic properties of the streams in the CCU plant. A flow diagram of the CCU plant is shown in Fig. 1.

4. Methodology

The CCU plant is evaluated using exergy, exergoeconomic, and exergoenvironmental analyses, the methodology of which is presented in the following sections.

4.1. Exergy analysis

Considering this presumption that there are no kinetic and potential energies, the exergy of a stream is divided into physical and chemical [29]. The physical exergy is the maximum available work generated by bringing a stream from its actual condition to the dead state expressed by P_0 and T_0. The physical exergy (e^{ph}) is calculated as[30]:

$$e^{ph} = (h - h_o) - T_o(s - s_o) \quad (1)$$

Where,h and s are the specific enthalpy and entropy, respectively. h_0 and s_0 are the enthalpy and entropy of the thermodynamic environment (h_0 =f (T_0, P_0) and s_0 =s (T_0, P_0)). The chemical exergy of an ideal mixture is [31]:

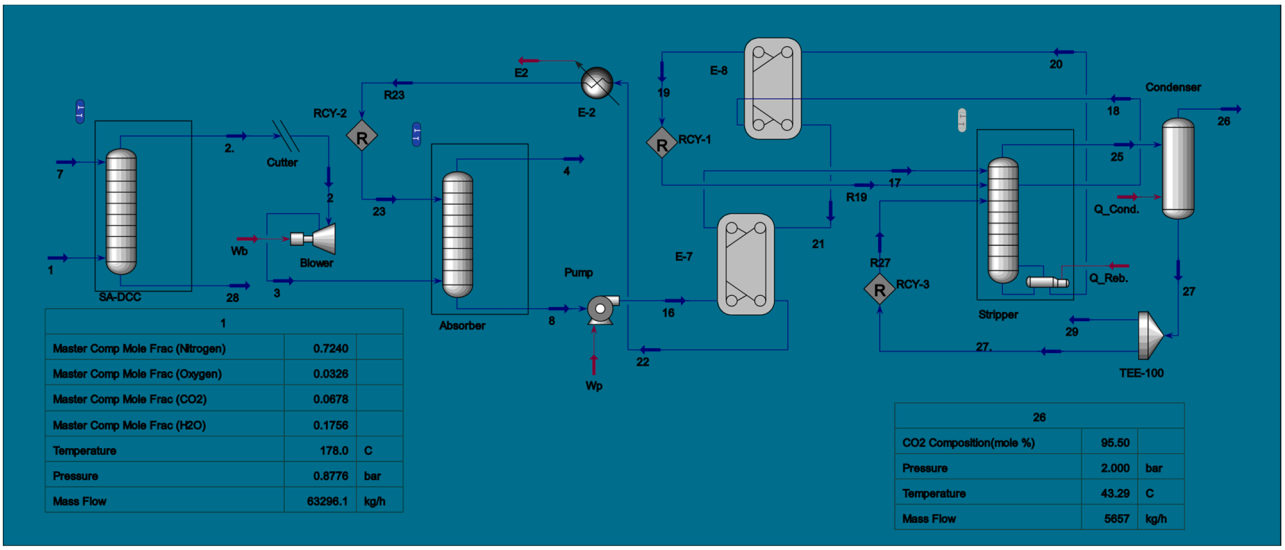

Fig. 1. Flowchart of the CCU plant.

Table 4
Physical and chemical exergy of streams.

Stream No.	Physical exergy (kW)	Chemical Exergy (kW)	Total Exergy (kW)
1	847.44	795.47	1642.91
2	58.49	571.74	630.22
3	127.21	571.74	698.94
4	86.25	164.67	250.92
7	64.21	5910.48	5974.69
8	167.58	4684.57	4852.15
16	176.08	4684.57	4860.65
17	669.09	4684.57	5353.67
18	1349.40	4576.11	5925.51
19	1657.92	4576.11	6234.02
20	1798.90	4547.77	6346.66
21	1408.68	4547.77	5956.44
22	653.23	4547.77	5200.99
23	114.97	4547.77	4662.74
25	197.60	733.68	931.28
26	76.96	671.03	747.99
27	0.75	62.65	63.40
28	306.04	6257.26	6563.30

Table 5
Exergy balances at the component level of the plant.

Component	Exergy of the fuel	**Exergy of the product**	**Exergy Destruction**
SA-DCC	$E_{F,SA-DCC} = E_1 + E_7 - E_{28}$	$E_{P,SA-DCC} = E_2$	$E_{D,SA-DCC} = E_{F,SA-DCC} - E_{P,SA-DCC}$
Blower	$E_{F,Blower} = W_b$	$E_{P,Blower} = E_3 - E_2$	$E_{D,Blower} = E_{F,Blower} - E_{P,Blower}$
Absorber	$E_{F,AB} = E_3 - E_4$	$E_{P,AB} = E_8 - E_{23}$	$E_{D,AB} = E_{F,AB} - E_{P,AB}$
Pump	$E_{F,Pump} = W_P$	$E_{P,Pump} = E_{16} - E_8$	$E_{D,Pump} = E_{F,Pump} - E_{P,Pump}$
Stripper	$E_{F,St} = E_{17} + E_{Q-Reb.}$	$E_{P,St} = E_{25} + E_{20} - E_{27} - E_{19}$	$E_{D,St} = E_{F,St} - E_{P,St}$
E-2	$E_{F,E-2} = E_{22} - E_{23}$	–	$E_{D,E-2} = E_{22} - E_{23} - E_{QE2}$
E-7	$E_{F,E-7} = E_{21} - E_{22}$	$E_{P,E-7} = E_{17} - E_{16}$	$E_{D,E-7} = E_{F,E-7} - E_{P,E-7}$
E-8	$E_{F,E-8} = E_{20} - E_{21}$	$E_{P,E-8} = E_{19} - E_{18}$	$E_{D,E-8} = E_{F,E-8} - E_{P,E-8}$
Condenser	$E_{F,Cond.} = E_{25} - E_{27} - E_{Q-Cond.}$	$E_{P,Cond.} = E_{26}$	$E_{D,E-8} = E_{F,Cond.} - E_{P,Cond.}$
Overall plant	$E_{F,tot} = E_{QE2} + W_P + W_B + E_{Q-Reb.} + E_{Q-Cond.}$	$E_{P,tot} = E_{26}$	$\dot{E}_{l,Total} = E_4 + E_{28} + E_{29} + E_{QE2}$ $E_{D,Total} = \Sigma E_{D,k}$

$$e^{ch} = \sum x_i e_0^i + T_0 R \sum x_i ln x_i \quad (2)$$

Where, x_i and e_0^i stand for the molar fraction and chemical exergy of each components existed in the mixture, and R stands for the universal gas constant [31]. Examples of standard chemical exergy values (kJ/mol) are 3.97 for O_2, 0.72 for N_2, 19.48 for CO_2, 337.9 for NH_3, and 900 for liquid H_2O, [32].

Exergy of a blend for real solutions can be obtained where activity coefficients, i.e., Υ_i are recognized for the components:

$$e^{ch} = \sum x_i e_0^i + T_0 R \sum x_i ln x_i \Upsilon_i \quad (3)$$

The total specific chemical exergy of a mixture can be calculated using the following equation.

$$e^{ch} = \sum x_i e_o^i \quad (4)$$

However, for a real mixture, intermolecular forces must be accounted for as well and the following equation can be used.

$$e^{ch} = \sum \left(x_i e_o^i\right) + \Delta G^{mix} \quad (5)$$

The Gibbs free energy ΔG^{mix} is estimated as follows:

$$\Delta G^{mix} = G - \sum x_i G_i \quad (6)$$

Table 4 shows the physical and chemical exergy of streams in the CCU plant.

The exergy efficiency is defined as the ratio of the useful exergy output ($\dot{E}_P$) to the total input exergy $\dot{E}_F$ [31]:

$$\varepsilon = \frac{\dot{E}_P}{\dot{E}_F} \quad (7)$$

The exergy destruction rate ($\dot{E}_{D,k}$) for an equipment is then calculated as:

$$\dot{E}_{D,k} = \dot{E}_{F,k} - \dot{E}_{P,k} \quad (8)$$

The exergy rate of heat transfer $\dot{Q}$ is [33]:

$$\dot{E}_Q = \dot{Q}\left(1 - \frac{T_0}{T}\right) \quad (9)$$

The definition of exergy of the fuel and product for each component is done and the exergy balances for the components of the system are presented in Table 5.

4.2. Exergoeconomic analysis

The economic assessment of the CCU plant is caried out via Aspen Process Economic Analyzer® (APEA). The capital costs typically include the purchased equipment cost (PEC) and their installation costs. The operational costs generally comprise of utility costs. APEA is a package to approximate costs of equipment and installation in a variety of processes [34]. By means of employing APEA in lieu of correlation-based economic methods implies that more parameters are taken into account to approximate the cost of equipment [35]. In this study, the project type "plant addition-adjacent to existing plant" is selected in the

Table 6
PEC and TDC of the process equipment.

Equipment tag	Equipment type ModMmtype	Equipment description	PEC/ (USD) U (USD)	TDC/ (USD)
SA-DCC (intercooler)	DHE PLAT FRAM	PFHE	14,000	126,600
SA-DCC	DTW PACKED	Packed tower	599,800	918,700
Stripper	DTW PACKED	Packed tower	294,400	530,300
Stripper (reboiler)	DRB U TUBE	TEMA shell and tube exchanger	73,400	177,400
Absorber	DTW PACKED	Packed tower	736,200	1,070,000
Absorber (intercooler)	DHE PLAT FRAM	PFHE	5000	89,900
Absorber (intercooler)	DHE PLAT FRAM	PFHE	3400	85,400
Absorber (intercooler)	DHE PLAT FRAM	PFHE	5000	89,900
Blower	EFN ROT BLOWER	Horizontal centrifugal	16,600	30,500
Pump	DCP CENTRIF	Horizontal centrifugal	10,000	60,300
E-2	DHE PLAT FRAM	PFHE	8900	115,100
Condenser	DVT CYLINDER	TEMA shell and tube exchanger	18,400	108,300
E-7	DHE PLAT FRAM	PFHE	9200	115,400
E-8	DHE PLAT FRAM	PFHE	9200	115,400

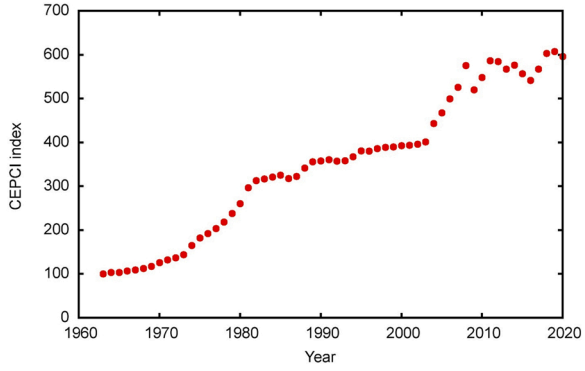

Fig. 2. CEPCI values in the years 1960–2020 [35].

Table 7
Cost rate balances and auxiliary equations for components of the proposed system.

Component	Cost rate equations	**Auxiliary equations**
SA-DCC	$\dot{C}_1 + \dot{C}_7 + \dot{Z}_{Ab.} = \dot{C}_2 + \dot{C}_{28}$	$c_1 = 0; c_7 = 0.21$ \$/GJ; $c_2 = c_{28}$
Blower	$\dot{C}_2 + \dot{C}_{W,\mathrm{blower}} + \dot{Z}_{\mathrm{blower}} = \dot{C}_3$	$c_{W,blower} = 21\$/\mathrm{GJ}$
Absorber	$\dot{C}_3 + \dot{C}_{23} + \dot{Z}_{Ab.} = \dot{C}_8 + \dot{C}_4$	$c_3 = c_4$
Pump	$\dot{C}_8 + \dot{C}_{W,Pump} + \dot{Z}_{Pump} = \dot{C}_{16}$	$c_{W,Pump} = 21\$/\mathrm{GJ}$
Stripper	$\dot{C}_{17} + \dot{C}_{19} + \dot{C}_{27} + \dot{C}_{TE} + \dot{Z}_{St.} = \dot{C}_{18} + \dot{C}_{20} + \dot{C}_{25}$	
E-7	$\dot{C}_{16} + \dot{C}_{21} + \dot{Z}_{E-7} = \dot{C}_{17} + \dot{C}_{22}$	$c_{22} = c_{21}$
E-8	$\dot{C}_{18} + \dot{C}_{20} + \dot{Z}_{E-8} = \dot{C}_{19} + \dot{C}_{21}$	$c_{20} = c_{21}$
E-2	$\dot{C}_{22} + \dot{Z}_{E-2} = \dot{C}_{23}$	–
Condenser	$\dot{C}_{25} + \dot{Z}_{Cond.} = \dot{C}_{26} + \dot{C}_{27}$	$c_{26} = c_{27}$

Table 8
Component balances of the exergoenvironmental analysis.

Component	Exergoenvironmental equations	**Auxiliary equations**
SA-DCC	$\dot{B}_1 + \dot{B}_7 + \dot{Y}_{Ab.} = \dot{B}_2 + \dot{B}_{28}$	$b_1 = 0; b_7 = 0 \quad ; b_2 = b_{28}$
Blower	$\dot{B}_2 + \dot{B}_{W,\mathrm{blower}} + \dot{Y}_{\mathrm{blower}} = \dot{B}_3$	$b_{W,blower} = 5050 mpt/\mathrm{GJ}$
Absorber	$\dot{B}_3 + \dot{B}_{23} + \dot{Y}_{Ab.} = \dot{B}_8 + \dot{B}_4$	$b_3 = b_4$
Pump	$\dot{B}_8 + \dot{B}_{W,Pump} + \dot{Y}_{Pump} = \dot{B}_{16}$	$b_{W,Pump} = 5050\mathrm{mpt/GJ}$
Stripper	$\dot{B}_{17} + \dot{B}_{19} + \dot{B}_{27} + \dot{B}_{TE} + \dot{Y}_{St.} = \dot{B}_{18} + \dot{B}_{20} + \dot{B}_{25}$	
E-7	$\dot{B}_{16} + \dot{B}_{21} + \dot{Y}_{E-7} = \dot{B}_{17} + \dot{B}_{22}$	$b_{22} = b_{21}$
E-8	$\dot{B}_{18} + \dot{B}_{20} + \dot{Y}_{E-8} = \dot{B}_{19} + \dot{B}_{21}$	$b_{20} = b_{21}$
E-2	$\dot{B}_{22} + \dot{Y}_{E-2} = \dot{B}_{23}$	–

Table 9
Allowed value ranges of decision variables.

Decision variables	Range
Lean MEA Temperature (°C)	[40–60]
Lean MEA Loading (mole CO_2/MEA)	[0.05–0.35]
Absorber packing height (m)	[5–14]
Stripper packing height (m)	[3–12]

APEA. The plant is designated to be located in Asia, and USD is the used currency. Table 6 presents the PEC and the total direct costs (TDC), including total material and manpower cost of the integrated CCU plant. The costs calculated using APEA are updated to the year 2020. The cost of intercoolers located in absorber and SA-DCC as well as reboiler in stripper are considered within the cost of correspondence column. Plate and Frame Heat Exchanger (PFHE) are employed for the main process heat exchangers as well as intercoolers.

As the system simulated by Aspen version 10 (2017); therefore, the cost must be updated. To update a given cost (original cost) to a reference year, the following equation can be used [36]:

$$Cost \quad at \quad reference \quad year = Original \quad Cost \times \frac{\mathrm{CEPCI}_{reference}}{\mathrm{CEPCI}_{Original}} \tag{10}$$

The Chemical Engineering Plant Cost Index (CEPCI) is an index widely used to update the equipment costs [37]. Fig. 2 shows the variation of CEPCI between 1960 and 2020.

The exergoeconomic balances are defined for each component k in the process and for the overall plant [38]:

$$\dot{C}_{\mathrm{F,k}} + \dot{Z}_{\mathrm{k}} - \dot{C}_{\mathrm{P,k}} = 0 \tag{11}$$

$\dot{C}_{\mathrm{F,k}}$, $\dot{C}_{\mathrm{P,k}}$, $\dot{C}_{\mathrm{D,k}}$ are associated costs related to fuel, product and destruction of a component; respectively. $\dot{Z}_K$ is the cost rate of component k and includes the capital investment and operation and maintenance costs ($\dot{Z}_{CI,K}$ and $\dot{Z}_{OM,K}$). Furthermore, $\dot{Z}_K$ because of inflation is being corrected to the reference year 2020 as follows [39]:

$$\dot{Z}_K = \frac{\mathrm{CEPCI}_{2020}}{\mathrm{CEPCI}_{2017}} \times \frac{CRF \times \varphi}{\tau} \times \mathrm{PEC}_K \tag{12}$$

$$CRF = \frac{i(1+i)^n}{(1+i)^n - 1} \tag{13}$$

Where CRF is the capital recovery factor, φ is the maintenance factor set at 1.06, τ stands for the annual operating hours considered to be 8000 h, i is the interest rate, assumed to be equal to 10%, and n is the number of total operational years equal to 20 years [39].

The specific cost of the exergy of the fuel exergy is the cost at which the exergy of the fuel is provided to the k_{th} component and calculated as [31]:

$$c_{F,K} = \dot{C}_{F,K} \Big/ \dot{E}_{F,K} \tag{14}$$

In the same way, the specific cost of the product of exergy is estimated as:

$$c_{P,K} = \dot{C}_{P,K} \Big/ \dot{E}_{P,K} \tag{15}$$

The cost rate of exergy destruction for each component, i.e., $\dot{C}_{D,K}$, is calculated multiplying the specific cost of the component with its exergy destruction calculated in a preceding exergetic analysis:

$$\dot{C}_{D,K} = c_{F,K}\dot{E}_{D,K} \tag{16}$$

Table 7 represents the overall cost balances and auxiliary equations assumed for each of equipment in the CCU plant. The cost rate associated with electrical power consumed in the blower and the pump of the CCU plant is assumed to be 21 $/GJ. The cost associated with thermal energy is equal to 2.89 $/GJ, and the cost of cooling with cooling water is considered equal to 0.21 $/GJ [35].

The relative cost difference r_k between the average cost of the unit product and fuel exergies is defined as:

$$r_k = \frac{C_{P,K} - C_{F,K}}{C_{F,K}} = \frac{1-\varepsilon_k}{\varepsilon_k} + \frac{\dot{Z}_k}{C_{F,K}\dot{E}_{P,K}} \tag{17}$$

The exergoeconomic factor, f_k, shows which percentage of the total cost is associated exclusively with the investment cost $\dot{Z}_k$.

$$f_k = \frac{\dot{Z}_k}{\dot{Z}_k + \dot{C}_{D,K}} \tag{18}$$

f_k offers a relative criterion to assess the economic performance of a component.

The sum of total costs associated with exergy destruction and investment of a component, $\dot{Z}_k + \dot{C}_{D,K}$, provides an objective way to

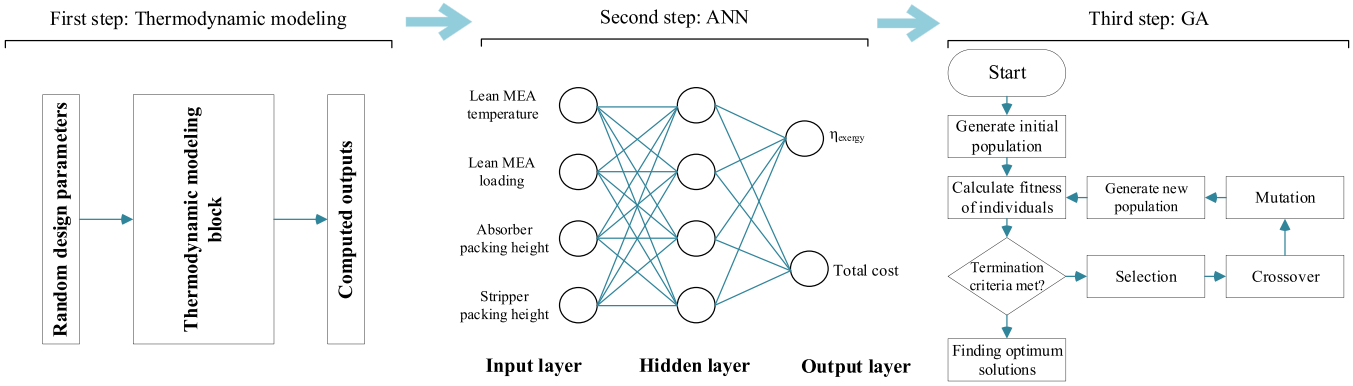

Fig. 3. Schematic of the optimization procedure.

Table 10
Results of the exergy analysis at the component level.

Component	$\varepsilon(\%)$	$E_{D,k}(kW)$	$E_{F,k}(kW)$	$E_{P,k}(kW)$
SA-DCC	59.78	424.07	1054.30	630.22
Blower	76.67	20.91	89.63	68.72
Absorber	42.28	258.61	448.02	189.41
Pump	61.75	5.26	13.76	8.50
Stripper	95.50	339.71	7554.25	7214.54
E-2	0.00	9.67	538.25	0.00
E-7	65.26	262.43	755.45	493.01
E-8	79.06	81.71	390.22	308.51
Condenser	78.50	222.22	1033.61	811.39
Overall plant	30.89	1673.73	2421.71	747.99

evaluate and rank the components based on their degree of importance. These values also reveal the components that should be looked at first in the optimization process following the analysis.

4.3. Exergoenvironmental analysis

The primary step to conduct an exergoenvironmental analysis is a life cycle assessment (LCA). LCA involves of (i) target and scope identification, (ii) inventory analysis, (iii) impact evaluation and (iv) interpretation [40]. The EI assessment can be carried out with different life cycle impact assessment (LCIA) methods; here the Eco-indicator 99 method is used [41]. The results using this indicator incorporate all of the impacts into one value expressed in eco-indicator points (Pts).

The exergoenvironmental analysis combines the exergy analysis with the preceding LCA. The goal with this analysis is to reveal the components and processes with the higher EI and find trade-offs between thermodynamic inefficiencies and EIs [42]. The EI of a material flow, Ḃj, expressed in eco-indicator units (Pts/s), is defined as:

$$\dot{B}_j = b_j \dot{E}_j \tag{19}$$

Where b_j stands for specific EI and $\dot{E}_j$ for exergy of the stream. The EI related of power and heat transfer are calculated by:

$$\dot{B}_w = b_w \dot{W} \tag{20}$$

$$\dot{B}_q = b_q \dot{E}_q \tag{21}$$

The EI balances are stated at the component level as [43]:

$$\dot{B}_{P,k} = \dot{B}_{F,k} + \dot{Y}_k \tag{22}$$

Where, $\dot{Y}_k$ is the EI of the construction of component k.

$$\dot{Y}_k = \dot{Y}_k^{CO} + \dot{Y}_k^{OM} + \dot{Y}_k^{DI} \tag{23}$$

Where, $\dot{Y}_k^{CO}$ includes the manufacturing, transport and installation of the component, $\dot{Y}_k^{OM}$ is the EI of operation and maintenance, $\dot{Y}_k^{DI}$ is the impact of the disposal of the component.

The exergoenvironmental evaluation is realized using some variables following similar practices as in the exergoeconomic analysis. First, the EI of exergy destruction is estimated as:

$$\dot{B}_{D,k} = b_{F,k} \dot{E}_{D,k} \tag{24}$$

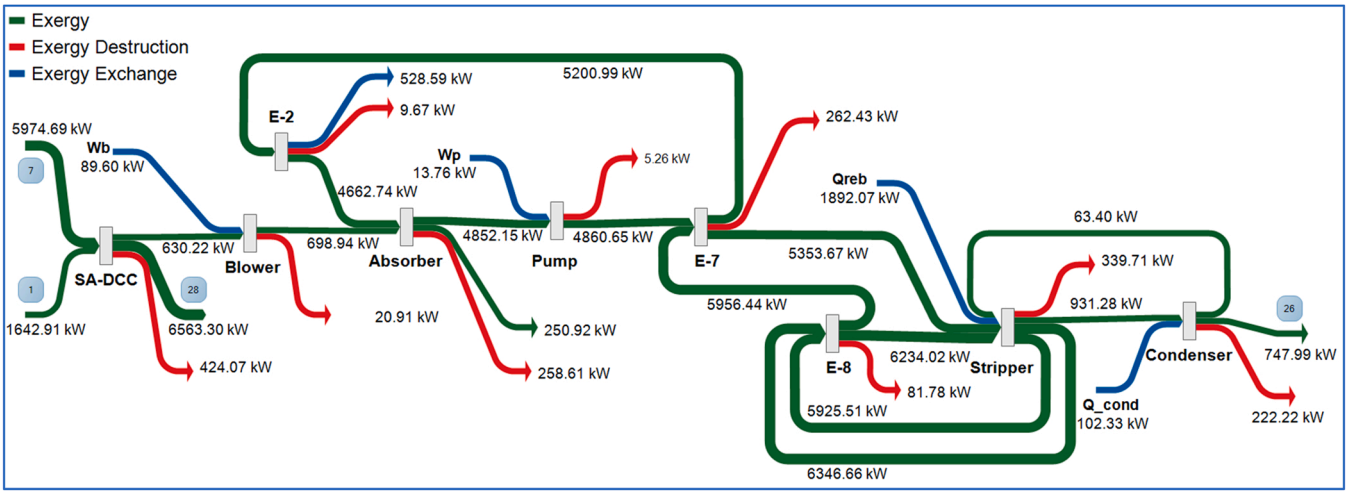

Fig. 4. Sankey diagram of exergy flows in the system.

Table 11
Exergy costs of streams.

Stream	c [$/GJ]	$\dot{C}$[$/h]
1	0	0.00
2	0.58	1.32
3	3.3	8.30
4	3.3	2.98
7	0.21	4.52
8	33.31	581.85
16	33.32	583.04
17	34.57	666.27
18	38.82	828.10
19	38.82	871.22
20	30.57	698.46
21	30.57	655.52
22	30.57	572.38
23	33.91	569.21
25	30.57	102.49
26	34.34	92.47
27	34.34	7.84
28	0.58	13.70

To reveal the most significant components from an EI viewpoint, the total EIs, $\dot{B}_{tot,k}$ is estimated:

$$\dot{B}_{tot,k} = \dot{Y}_k + \dot{B}_{D,k} \tag{25}$$

The relative difference of EIs, $r_{b,k}$, is an indicator of the reduction potential of the EI of a component:

$$r_{b,k} = \frac{b_{P,k} - b_{F,K}}{b_{F,K}} = \frac{1-\varepsilon_k}{\varepsilon_k} + \frac{\dot{Y}_k}{\dot{B}_{D,k}} \tag{26}$$

The exergoenvironmental factor, $f_{b,k}$, presents the relative contribution of the EI linked with the construction of a component to the sum of its EIs, and it is calculated as:

$$f_{b,k} = \frac{\dot{Y}_k}{\dot{Y}_k + \dot{B}_{D,k}} \tag{27}$$

Table 8 shows the component balances of the exergoenvironmental analysis. The EI rate of electrical power used in the blower and the pump of the system is assumed to be 5.05 mPts/MJ (obtained from SimaPro software as medium voltage {IR}| market for | APOS, U). The EI rate of the thermal energy of the steam used in the regeneration of the solvent is assumed to be 9.86 mPt/kg (obtained from SimaPro as Steam, in chemical industry {RoW}| market for steam, in chemical industry | APOS, U). The used steam with its given pressure and temperature has an enthalpy of 2.745 MJ/kg. As a result, its EI is equal to 3.592 mPts/MJ. The EI of the cooling water is assumed to be zero [44].

5. Optimization

Genetic algorithm (GA) among evolutionary optimization approaches is extensively employed in the design of neural networks due to the exceptional capability of finding a global optimum in multi-modal and/or non-differentiable search space. Training of neural networks by means of associated weights or coefficients generally are executed by such aforementioned stochastic methods. These methods normally perform better than traditional gradient-based techniques [45].

In this study, a multi-objective optimization problem is being solved. The objectives are to minimize the total cost rate and maximize the exergy efficiency. Two single-objective GAs and a NSGAII two-objective GA are used to obtain the optimum values[46]. For this goal, design variables are selected from both design and process operating conditions. The considered decision variables are the lean MEA temperature and loading, and the heights of the absorber and stripper. The design space for the GA is based on the values reported in [47]. The studied range values of the decision variables are listed in Table 9.

The objective function is anticipated with the trained ANN, instead of solving sets of equations. In this way, the running time of the optimization process is decreased significantly for each optimization execution [48]. The modeling procedure is repeated 100 times based on 100 random sets of input data. Next the output data are trained by the ANN. Fig. 3 shows the schematic of the optimization procedure.

6. Results and discussion

6.1. Exergy analysis results

After the simulation of the CCU plant and the calculation of the exergy of the involved material streams, the results of the analysis are presented in Table 10 and Fig. 4. It is seen that the main part of the exergy is destructed in the SADCC, the stripper and the absorber columns, with absolute amounts of 424.07, 339.71, and 258.61 kW, respectively. The exergy destruction within the CO_2 stripper is linked to chemical reactions and separation, as well as the considerable thermal energy loss in the inter coolers of the absorber and SADCC columns.

Table 13
LCA of the plant components.

Equipment	Material	ECO 99 (mPts/kg)	Weight (kg)	Total (mPts)	Yk (mPts/s)
SA-DCC	Stainless steel	1220	27,950	34,099,000	0.0540
Blower	Stainless steel	1220	3606	4,399,320	0.0070
Absorber	Stainless steel	1220	62,350	76,067,000	0.1205
Pump	Stainless steel	1220	525	640,500	0.0010
Stripper	Stainless steel	1220	25,450	31,049,000	0.0492
E-2	Stainless steel	1220	2531	3,087,820	0.0049
E-7	Stainless steel	1220	2693	3,285,460	0.0052
E-8	Stainless steel	1220	2703	3,297,660	0.0052
Condenser	Stainless steel	1220	2071	2,526,620	0.0040

Table 12
Results of the exergoeconomic analysis.

Equipment	$\dot{Z}(\$/h)$	$C_P(\$/GJ)$	$C_F(\$/GJ)$	$\dot{C}_D(\$/h)$	$\dot{E}_D(GJ/h)$	$\dot{Z} + \dot{C}_D(\$/h)$	r_k(%)	f_k(%)
SA-DCC	10.30	1.32	0.00	0.00	1.53	10.30	100	100.00
Blower	0.28	28.24	21.00	1.58	0.08	1.86	34.50	15.05
Absorber	12.60	18.54	3.30	3.07	0.93	15.67	461.82	80.40
Pump	0.17	39.03	21.00	0.40	0.02	0.57	85.86	29.94
Stripper	6.20	30.54	26.81	32.79	1.22	38.99	13.90	15.90
E-2	0.15	0.00	1.64	0.06	0.03	0.21	-	72.48
E-7	0.15	46.89	30.57	28.88	0.94	29.03	53.40	0.52
E-8	0.15	38.82	30.57	8.99	0.29	9.14	26.99	1.64
Condenser	0.32	34.34	27.83	22.26	0.80	22.58	23.39	1.42

Table 14
Component-level results of the exergoenvironmental analysis.

Equipment	$b_{F,k}$ $(mPts/GJ)$	$b_{P,k}$ $(mPts/GJ$	$\dot{B}_{D,k}$ $(mPts/\mathrm{hr})$	$\dot{Y}_k$ $(mPts/\mathrm{hr})$	$\dot{B}_{Tot,k}$ $(mPts/hr)$	$r_{b,k}$ (%)	$f_{b,k}$ (%)
SA-DCC	0.00	17.0319	0.00	194.50	194.50	-	-
Blower	5050.00	6634.70	380.16	25.09	405.25	31.4	6.19
Absorber	659.10	723.03	613.62	433.88	1047.50	9.7	41.42
Pump	5050.00	8939.95	95.68	3.65	99.33	77.0	3.67
Stripper	27193.23	31230.94	33256.30	177.10	33433.40	14.8	0.53
E-2	16.60	0.00	0.58	17.61	18.19	-	-
E-7	31263.00	47893.10	29536.01	18.74	29554.75	53.2	0.06
E-8	31263.00	39588.00	9195.79	18.81	9214.60	26.6	0.20
Condenser	28168.10	34911.00	22534.30	14.41	22548.71	23.9	0.06

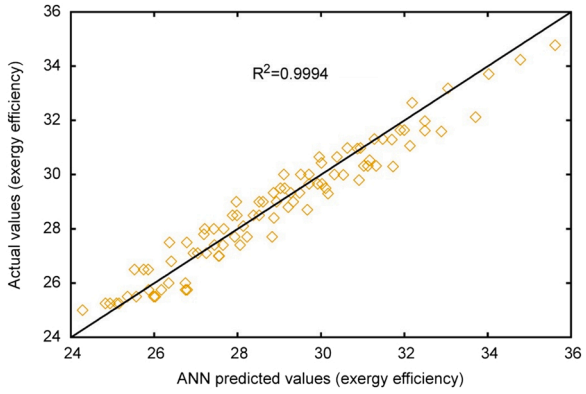

Fig. 5. Coefficient of determination of the exergy efficiency.

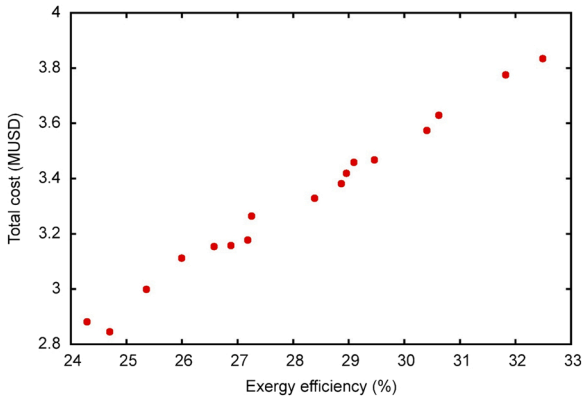

Fig. 6. The Pareto front and selected optimal points.

Among the heat exchangers included in the process, the heat exchangers E-7 and E-8 result in the largest amounts of exergy destruction equal to 262.43 and 81.71 kW, respectively. These are heat exchangers needed between the absorber and stripper columns and their use cannot be avoided. Although in PCC system it is common to use one heat exchangers between these columns, in this system two-stage heat exchanger is used to enhance the CO_2 stripping. Heat exchanger E-2 is considered dissipative because it has no useful product. The generated thermal energy here is exhausted and not further used. The condenser also results in a considerable amount of exergy destruction, with the value of 222.22 kW.

6.2. Exergoeconomic analysis results

Table 11 presents unit the exergy cost and cost rates for each material stream in the CCU plant. The cost of the feeding stream, i.e., the flue gas from ammonia plant is considered zero. As seen, the cost rate of captured CO_2 from the CCU plant increases when passing through the equipment of the system, particularly in the case of the compressors that are driven by electricity.

After carrying out the exergy and exergoeconomic analysis, the operation and evaluation of the individual components takes place. The results of the mentioned parameters are presented in Table 12.

The significance of each component is revealed from the scale of its total costs, $\dot{Z}_k + \dot{C}_{D,K}$. The components are consequently ranked in importance based on that cost, with the components with highest values ranked first. The highest sum of costs is calculated for the CO_2 stripper, followed by the heat exchanger E-7. The exergoeconomic factor shows the contribution of the investment cost on the total cost. When the f_k is high, a decrease of the investment cost of the component should, most probably, be considered. High exergoeconomic factors are calculated for the SADCC and absorber columns. A reduction thus of their investment cost could be a way to improve the exergoeconomic performance of the plant. A low f_k, shows a high exergy destruction that implies that the thermodynamic performance of the component should be considered. In this study, low values of the exergoeconomic factor are calculated for the process heat exchangers.

6.3. Resutls of the exergoenvironmental analysis

To calculate the EI of each component in the process, the material type and weights of each used material need to be known or accordingly calculated. The LCA of the components of the CCU plant is shown in Table 13. Overall, the absorber column is found to have the largest EI, equal to approximately 0.1205 mPt/s.

Table 14 presents the results of the exergoenvironmental analysis. It can be seen that the largest part of the total EI of the system stems from the exergy destruction of the components. The highest EI of exergy destruction, equal to 33,256.3 mPts/hr, is calculated for the stripper. This is mainly linked to the significant use of steam in the reboiler of the stripper. The exergoenvironmental factors are generally found to be relatively low, with the exception of the absorber. This shows that the EI associated with the components is negligible when compared to that of the exergy destruction.

6.4. Optimization results

In order to verify that the ANN has been adequately and appropriately trained, its results are compared to those of the actual modeling. R-squared, R^2, (the coefficient of determination) is considered to measure the performance of the ANN model. How close the coefficient of determination of the exergy efficiency is to the actual values calculated, as shown in Fig. 5, shows the reliability of the generated ANN model.

The cost functions in a multi-objective optimization may lead to tradeoffs in optimization, where the improvement of one may lead to poorer performance of another. Since this is the case here, the Pareto front is used in the optimization efforts. Fig. 6 shows the Pareto front obtained from the multi-objective optimization problem. As mentioned, the objective functions for optimization are the maximization of the exergy efficiency and the minimization of the total cost rate. The

solutions on a Pareto front are non-dominant and each of these solutions may be selected as the optimum solution depending on designer's preferences. Nevertheless, a solution providing the best trade-off among the different objective functions is commonly of interest.

7. Conclusion

In this work, the exergoeconomic and exergoenvironmental evaluation, as well as a multi-objective optimization are carried out for a CO_2 utilization plant. The plant is developed and simulated in Aspen Hysys™ v.10 software and results in an overall exergy efficiency equal to 30.89%. The exergy analysis reveals that the main part of the exergy is destroyed in the SADCC, the stripper and the absorber columns, with values equal to 424.07, 339.71, and 258.61 kW, respectively. The exergoeconomic analysis shows that the process heat exchangers of the system, specifically E-7 and E-8, result in relatively low value of the exergoeconomic factor i.e., 0.52 and 1.64 respectively, while, on the other hand, high values of the factor are calculated for the SADCC and the absorber columns with the amounts of 100% and 80.4%. It is seen thus that an improvement in the thermodynamic performance of the heat exchangers and a decrease in the investment cost of the SADCC and absorber should be considered to improve the overall exergoeconomic performance of the system.

The data obtained from the simulation of the plant have been used to train an artificial neural network that is then used with a genetic algorithm to optimize the plant, by minimizing the total costs and maximizing the efficiency. Relevant decision variables were the lean monoethanolamine temperature and loading, and the heights of the absorber and the stripper. The results of the life cycle assessment shows that the absorber column has the largest EI, while the highest EI of exergy destruction is estimated for the stripper of the plant.

CRediT authorship contribution statement

Reza Shirmohammadi: Conceptualization, Methodology, Software, Formal analysis, Visualization, Writing – original draft, Writing – review & editing.**Alireza Aslani**: Project administration, Supervision, Resources, Writing – review & editing. **Roghayeh Ghasempour**: Project administration, Supervision, Resources, Writing – review & editing. **Luis M. Romeo**: Supervision, Writing – review & editing. **Fontina Petrakopoulou**: Supervision, Methodology, Writing – review & editing.

Declaration of Competing Interest

The authors declare that they have no known competing financial interests or personal relationships that could have appeared to influence the work reported in this paper.

Acknowledgments

Reza Shirmohammadi would like to acknowledge both the Iran's National Elite Foundation (INEF) for the financial support [grant number 15.20772] and the University of Tehran for providing support at this work. The technical supports of the Kermanshah Petrochemical Industries Co. and Shahrekord Carbon Dioxide Co. are gratefully acknowledged. Fontina Petrakopoulou would like to thank the Spanish Ministry of Science, Innovation and Universities, and the Universidad Carlos III de Madrid (Ramón y Cajal Programme, RYC-2016-20971).

References

[1] J.E. Bistline, V.J.Ep Rai, The role of carbon capture technologies in greenhouse gas emissions-reduction models: a parametric study for the US power sector, Energy Policy 38 (2) (2010) 1177–1191.
[2] M. Bailera, P. Lisbona, B. Peña, L.M. Romeo, A review on CO_2 mitigation in the Iron and Steel industry through Power to X processes, J. CO2 Util. 46 (2021), 101456.
[3] H. Nasrollahi, F. Ahmadi, M. Ebadollahi, S. Najafi Nobar, M. Amidpour, The greenhouse technology in different climate conditions: a comprehensive energy-saving analysis, Sustain. Energy Technol. Assess. 47 (2021), 101455.
[4] F. Petrakopoulou, G. Tsatsaronis, Can carbon dioxide capture and storage from power plants reduce the environmental impact of electricity generation? Energy Fuels 28 (8) (2014) 5327–5338.
[5] D. Iribarren, F. Petrakopoulou, J. Dufour, Environmental and thermodynamic evaluation of CO_2 capture, transport and storage with and without enhanced resource recovery, Energy 50 (2013) 477–485.
[6] Z. Amrollahi, I.S. Ertesvåg, O. Bolland, Optimized process configurations of post-combustion CO 2 capture for natural-gas-fired power plant—Exergy analysis, Int. J. Greenh. Gas. Control 5 (6) (2011) 1393–1405.
[7] Z. Zhou, Z. You, Z. Wang, X. Hu, J. Zhou, K. Cen, Process design and optimization of state-of-the-art carbon capture technologies, Environ. Prog. Sustain. Energy 33 (3) (2014) 993–999.
[8] L.M. Romeo, D. Minguell, R. Shirmohammadi, J.M. Andrés, Comparative analysis of the efficiency penalty in power plants of different amine-based solvents for CO_2 capture, Ind. Eng. Chem. Res. 59 (21) (2020) 10082–10092.
[9] L.M. Romeo, P. Lisbona, Y. Lara, Combined carbon capture cycles: an opportunity for size and energy penalty reduction, Int. J. Greenh. Gas. Control 88 (2019) 290–298.
[10] F. Petrakopoulou, G. Tsatsaronis, A. Boyano, T. Morosuk, Post-combustion CO_2 Capture with Monoethanolamine in a Combined-cycle Power Plant: Exergetic, Economic and Environmental Assessment, Greenhouse Gases–Emission, Measurement and Management, InTech–Open Access Company,, 2012.
[11] L.E. Øi, Aspen HYSYS Simulation of CO_2 Removal by Amine Absorption from a Gas Based Power Plant, The 48th Scandinavian Conference on Simulation and Modeling (SIMS 2007); 30-31 October; 2007; Göteborg (Särö), Linköping University Electronic Press, 2007, pp. 73–81.
[12] R. Shirmohammadi, M. Soltanieh, L.M. Romeo, Thermoeconomic analysis and optimization of post-combustion CO_2 recovery unit utilizing absorption refrigeration system for a natural-gas-fired power plant, Environ. Prog. Sustain. Energy 37 (3) (2018) 1075–1084.
[13] G. Ferrara, A. Lanzini, P. Leone, M. Ho, D. Wiley, Exergetic and exergoeconomic analysis of post-combustion CO_2 capture using MEA-solvent chemical absorption, Energy 130 (2017) 113–128.
[14] F.H. Geuzebroek, L.H.J.M. Schneiders, G.J.C. Kraaijveld, P.H.M. Feron, Exergy analysis of alkanolamine-based CO_2 removal unit with AspenPlus, Energy 29 (9) (2004) 1241–1248.
[15] Z. Amrollahi, I.S. Ertesvåg, O. Bolland, Optimized process configurations of post-combustion CO_2 capture for natural-gas-fired power plant—exergy analysis, Int. J. Greenh. Gas. Control 5 (6) (2011) 1393–1405.
[16] Y.S. Yu, Y. Li, Q. Li, J. Jiang, Z.X. Zhang, An innovative process for simultaneous removal of CO_2 and SO2 from flue gas of a power plant by energy integration, Energy Convers. Manag. 50 (12) (2009) 2885–2892.
[17] B. Wang, H. Jin, D. Zheng, Recovery of CO_2 with MEA and K2CO3 absorption in the IGCC system, Int. J. Energy Res. 28 (6) (2004) 521–535.
[18] F. Petrakopoulou, G. Tsatsaronis, T. Morosuk, Evaluation of a power plant with chemical looping combustion using an advanced exergoeconomic analysis, Sustain. Energy Technol. Assess. 3 (2013) 9–16.
[19] Y. Lara, A. Martínez, P. Lisbona, I. Bolea, A. González, L.M. Romeo, Using the second law of thermodynamic to improve CO 2 capture systems, Energy Procedia 4 (2011) 1043–1050.
[20] K. Atsonios, K. Panopoulos, P. Grammelis, E. Kakaras, Exergetic comparison of CO 2 capture techniques from solid fossil fuel power plants, Int. J. Greenh. Gas. Control 45 (2016) 106–117.
[21] M. Gatti, E. Martelli, F. Marechal, S. Consonni, Review, modeling, heat integration, and improved schemes of Rectisol®-based processes for CO 2 capture, Appl. Therm. Eng. 70 (2) (2014) 1123–1140.
[22] G. Valenti, D. Bonalumi, E. Macchi, Energy and exergy analyses for the carbon capture with the Chilled Ammonia Process (CAP), Energy Procedia 1 (1) (2009) 1059–1066.
[23] O.J. Odejobi, C.F. Jisieike, A.N. Anozie, Simulation and exergy analysis of processes for CO_2 capture and utilisation for methanol production, Int. J. Exergy 17 (4) (2015) 456–474.
[24] F. Yulia, R. Sofianita, K. Prayogo, N. Nasruddin, Optimization of post combustion CO_2 absorption system monoethanolamine (MEA) based for 320 MW coal-fired power plant application – Exergy and exergoenvironmental analysis, Case Stud. Therm. Eng. 26 (2021), 101093.
[25] R. Shirmohammadi, A. Aslani, R. Ghasempour, Challenges of carbon capture technologies deployment in developing countries, Sustain. Energy Technol. Assess. 42 (2020), 100837.
[26] L. Dubois, D. Thomas, Comparison of various configurations of the absorption-regeneration process using different solvents for the post-combustion CO_2 capture applied to cement plant flue gases, Int. J. Greenh. Gas. Control 69 (2018) 20–35.
[27] R. Shirmohammadi, A. Aslani, R. Ghasempour, L.M. Romeo, CO_2 Utilization via Integration of an Industrial Post-Combustion Capture Process with a Urea Plant: Process Modelling and Sensitivity, Anal., Process. 8 (9) (2020) 1144.
[28] R. Shirmohammadi, A. Aslani, R. Ghasempour, L.M. Romeo, F. Petrakopoulou, Techno-economic assessment and optimization of a solar-assisted industrial post-combustion CO_2 capture and utilization plant, Energy Rep. 7 (2021) 7390–7404.
[29] A. Abdollahpour, R. Ghasempour, A. Kasaeian, M.H. Ahmadi, Exergoeconomic analysis and optimization of a transcritical CO_2 power cycle driven by solar energy based on nanofluid with liquefied natural gas as its heat sink, J. Therm. Anal. Calorim. 139 (1) (2020) 451–473.

[30] B.S. Bagheri, R. Shirmohammadi, S.M.S. Mahmoudi, M.A. Rosen, Optimization and comprehensive exergy-based analyses of a parallel flow double-effect water-lithium bromide absorption refrigeration system, Appl. Therm. Eng. 152 (2019) 643–653.
[31] A. Bejan, G. Tsatsaronis, M. Moran, M.J. Moran, Thermal Design and Optimization, John Wiley \& Sons, 1996.
[32] J. Szargut, Egzergia: Poradnik Obliczania i Stosowania, Wydawnictwo Politechniki Śląskiej, 2007.
[33] A. Mahmoudan, P. Samadof, M. Sadeghzadeh, M. Jalili, M. Sharifpur, R. Kumar, Thermodynamic and exergoeconomic analyses and performance assessment of a new configuration of a combined cooling and power generation system based on ORC–VCR, J. Therm. Anal. Calorim. (2020).
[34] J. Haydary, Chemical Process Design and Simulation: Aspen Plus and Aspen Hysys applications, John Wiley & Sons, 2019.
[35] R. Shirmohammadi, A. Aslani, R. Ghasempour, L.M. Romeo, F. Petrakopoulou, Process design and thermoeconomic evaluation of a CO_2 liquefaction process driven by waste exhaust heat recovery for an industrial CO_2 capture and utilization plant, J. Therm. Anal. Calorim. (2021).
[36] Z. Liu, Z. Liu, X. Yang, H. Zhai, X. Yang, Advanced exergy and exergoeconomic analysis of a novel liquid carbon dioxide energy storage system, Energy Convers. Manag. 205 (2020), 112391.
[37] P. Charoensuppanimit, K. Kitsahawong, P. Kim-Lohsoontorn, S. Assabumrungrat, Incorporation of hydrogen by-product from NaOCH3 production for methanol synthesis via CO_2 hydrogenation: process analysis and economic evaluation, J. Clean. Prod. 212 (2019) 893–909.
[38] A. Ekrataleshian, F. Pourfayaz, M.H. Ahmadi, Thermodynamic and thermoeconomic analyses and energetic and exergetic optimization of a turbojet engine, J. Therm. Anal. Calorim. (2020).
[39] Z. Liu, T. He, Exergoeconomic analysis and optimization of a Gas Turbine-Modular Helium Reactor with new organic Rankine cycle for efficient design and operation, Energy Convers. Manag. 204 (2020), 112311.
[40] A. Keçebaş, Exergoenvironmental analysis for a geothermal district heating system: an application, Energy 94 (2016) 391–400.
[41] M.J. Goedkoop, The Eco-indicator 99 a damage oriented method for life cycle impact assessment methodology report, Pre Concultants (1999).
[42] F. Petrakopoulou, G. Tsatsaronis, A. Boyano, T. Morosuk, Exergoeconomic and exergoenvironmental evaluation of power plants including CO_2 capture, Chem. Eng. Res. Des. 89 (9) (2011) 1461–1469.
[43] L. Meyer, G. Tsatsaronis, J. Buchgeister, L. Schebek, Exergoenvironmental analysis for evaluation of the environmental impact of energy conversion systems, Energy 34 (1) (2009) 75–89.
[44] E.J.C. Cavalcanti, Exergoeconomic and exergoenvironmental analyses of an integrated solar combined cycle system, Renew. Sustain. Energy Rev. 67 (2017) 507–519.
[45] R. Shirmohammadi, B. Ghorbani, M. Hamedi, M.-H. Hamedi, L.M. Romeo, Optimization of mixed refrigerant systems in low temperature applications by means of group method of data handling (GMDH), J. Nat. Gas. Sci. Eng. 26 (2015) 303–312.
[46] B. Ghorbani, R. Shirmohammadi, M. Mehrpooya, M.-H. Hamedi, Structural, operational and economic optimization of cryogenic natural gas plant using NSGAII two-objective genetic algorithm, Energy 159 (2018) 410–428.
[47] A.S. Lee, J.C. Eslick, D.C. Miller, J.R. Kitchin, Comparisons of amine solvents for post-combustion CO_2 capture: a multi-objective analysis approach, Int. J. Greenh. Gas. Control 18 (2013) 68–74.
[48] M.A. Emadi, J. Mahmoudimehr, Modeling and thermo-economic optimization of a new multi-generation system with geothermal heat source and LNG heat sink, Energy Convers. Manag. 189 (2019) 153–166.